Influence of Oxidation in Starting Material Sn on Electric Transport Properties of SnSe Single Crystals

Aichi Yamashita[1, 2‡], Osamu Ogiso[1, 2], Ryo Matsumoto[1, 2], Masashi Tanaka[1, 3],

Hiroshi Hara[1, 2], Hiromi Tanaka[4], Hiroyuki Takeya[1], Chul-Ho Lee[5], and

Yoshihiko Takano[1, 2]

[1] WPI-MANA, National Institute for Materials Science, 1-2-1 Sengen, Tsukuba, Ibaraki,

305-0047, Japan

[2] Graduate School of Pure and Applied Sciences, University of Tsukuba, 1-1-4

Tennodai, Tsukuba, Ibaraki, 305-8577, Japan

[3] Graduate School of Engineering, Kyushu Institute of Technology, 1-1 Sensui-cho,

Tobata, Kitakyushu, Fukuoka, 804-8550, Japan

[4] National Institute of Technology, Yonago College, 4448 Hikona, Yonago, Tottori 683-

8502, Japan

[5] National Institute of Advanced Industrial Science and Technology (AIST), Tsukuba,

Ibaraki, 305-8568, Japan

We found that the electronic transport property of SnSe single crystals was sensitively

affected by oxidation in raw Sn. Semiconducting SnSe single crystals were obtained by

19   using Sn of grain form as a starting material while powder Sn resulted in metallic SnSe.

20   X-ray photoelectron spectroscopy analysis revealed that the surfaces of raw Sn were

21   oxidized, which volume fraction is lower in grain Sn. This indicates that the amount of

22   oxygen in raw Sn is the key factor for the electronic transport property of SnSe.

23   SnSe is well-known as a p-type semiconductor for a long time [1-3]. Recently, Zhao et

24   al. reported that SnSe single crystal shows ultrahigh dimensionless figure-of-merit (ZT)

25   values of 2.6 and 2.3 at 923 K in the b and c directions [4]. These high ZT values are

26   achieved with high power factor and extremely low thermal conductivity. After the report

27   in 2014, intense investigations have been conducted by many groups [5-22]. More

28   recently, the ZT values around 2.0 have been reported with Bi-doped n-type and Na-doped

29   p-type SnSe single crystals [5, 16, 17]. However, the reproducibility of the exceptionally

30   high thermoelectric performance has not been obtained to date. Different thermoelectric

31   properties, especially in electrical conductivity, have been reported from several groups

32   for both of single crystalline and poly crystalline samples. Some groups reported metallic

33   behavior in electrical conductivity [16-18]. On the other hand, others reported

34   semiconducting behavior [19-23] and consistent results have not been obtained so far.

35   Motivated to figure out the reason of these different results, we focused on the possible

36   influence of oxygen content in the starting materials of Sn. Herein, we report on the

37   electrical conductivity measurements along the bc plane for SnSe single crystals in a

38   temperature range from 2 to 390 K. It was found that the electrical conductivity was

39   controlled by changing the oxygen content during the synthesis. The electrical conducting

40   behavior changed from semiconducting to metallic with increase of the oxygen content

41   in the raw Sn.

42   Single crystals of SnSe were grown from the congruent melt. Starting materials were

43   Se chips and two different forms of Sn. Grain form Sn (diameter: ~ 3.0 mm) and powder

44   form Sn (diameter: ~ 0.15 mm) with the same purity of 99.99 % were used. To examine

45   the form dependence on electric transport property of grown single crystals, the ratio of

46   grain and powder form Sn was systematically varied (grain Sn : powder Sn = 100 : 0, 90 :

47   10, 70 : 30, 0 : 100). These Sn grains and/or Sn powders and Se chips were loaded into

48   quartz tubes in stoichiometric composition. The tubes were then evacuated and sealed.

49   They were slowly heated to 600°C and kept for 12 hours followed by furnace cooling. As

50   a result, poly crystalline ingot of SnSe was obtained. The obtained ingot was ground and

51   heated to 1000°C and kept for 10 hours in the double sealed evacuated quartz tubes. These

52   double quartz tubes are necessary to avoid the enters of the oxygen by the breaks of inner

53   quartz tube due to stress from the structural transition during furnace cooling. They were

54   cooled down to 840°C in 8 hours followed by furnace cooling. Finally, SnSe single

55   crystals with typical size of $10 \times 5 \times 3$ mm^3 were obtained.

56   Powder X-ray diffraction (XRD) patterns were measured by using Mini Flex 600

57   (Rigaku) with Cu-Kα radiation. For the measurements, single crystals were ground into

58   powder. Chemical states of raw Sn were examined by X-ray photoelectron spectroscopy

59 (XPS) analysis using an AXIS-ULTRA DLD (Shimadzu/Kratos) with an Al-Kα X-ray

60 radiation (hv = 1486.6 eV), operating at a pressure of 9×10^{-9} Torr. The analyzed area

61 was approximately 1×1 mm^2. Electrical conductivity was measured using a Physical

62 Properties Measurements System (PPMS, Quantum Design) in the temperature range of

63 2–390 K.

64 XPS analysis was carried out to examine the chemical states of raw Sn in the both grain

65 (red line) and powder (blue line) forms (Fig.1). There is a well-defined peak at 487.5 eV

66 in the XPS spectrum of the Sn 3d, which is associated with the Sn 3d$_{5/2}$ state. This is a

67 characteristic feature of a tetravalent Sn ion (Sn^{4+}) [24], implying the presence of SnO$_2$

68 in both grain and powder Sn. Most likely, it could be on the surfaces. The smaller peak at

69 around 485 eV arises from the Sn^0 state [24], indicating the presence of the non-oxidized

70 metal Sn. The thickness of SnO$_2$ layer should be less than few nm that is the value of the

71 penetration depth of XPS measurement. These results indicate that by using the powder

72 Sn the larger amount of oxygen content would be included during the synthesis due to

73 larger volume fraction of SnO$_2$ coming from the larger surface area.

74 Figure 2 shows the X-ray diffraction patterns of pulverized SnSe single crystals grown

75 from grain and powder Sn. Inset shows the enlargement of the (400) reflection. The

76 diffraction patterns of both samples can be indexed with an orthorhombic system of the

77 space group *Pnma*. The lattice constants of *a*, *b* and *c* axes were determined to be $a =$

78 11.48(7) Å, $b = 4.44(2)$ Å and $c = 4.15(1)$ Å for both samples comparable to the literature.

79 Note that there are no peaks related to SnO_2, indicating that the oxygen content is quite

80 low.

81 Figure 3 shows the temperature dependence of the electrical conductivity of SnSe single

82 crystals along the *bc* plane. The electrical conductivity strongly depends on the ratio of

83 grain and powder form Sn used as starting materials. The sample from grain Sn 100%,

84 which may contain the smallest amount of oxygen content, showed semiconducting

85 behavior. The conductivity sharply decreased with decreasing temperature. The small

86 electrical conductivity indicates a low hole concentration ensuring the purity of the

87 sample that has small deviation from the ideal stoichiometry. On the other hand, the

88 electrical conductivities increased and their behaviors became metal like with decreasing

89 the ratio of grain Sn and increasing the amount of oxygen content. The electrical

90 conductivity of SnSe grown by 100% powder Sn showed good agreement with that of the

91 reported ones by Zhao et al. [4]. The present results indicate that transport properties of

92 SnSe single crystal can be controlled from semiconductor to metal by varying the ratio of

93 grain and powder form of Sn used as a starting material. This can be due to the difference

94 of the oxygen volume fraction presenting on the surface of both raw Sn. In fact, pure SnSe

95   is known as a p-type semiconductor [1-3], which is in good agreement with our

96   semiconducting SnSe single crystals with the lowest amount of oxygen content. Hole

97   carrier can be doped by the lack of Sn [1]. Our metallic SnSe could also be explained by

98   the increase of hole carrier with increasing the Sn deficiency, which can be caused by the

99   deviation from the stoichiometry due to the oxidization of the surface of raw Sn. In any

100   case the existence of oxygen plays the important role to change the electronic state of

101   SnSe, possibly by interacting with a lone pair or existing in an interstitial site, and so on.

102   Further investigation on the mechanism of oxygen effect for electrical conduction would

103   be important for the comprehension of intrinsic properties of SnSe.

104   We found that the different electrical conductivity reported by several groups could be

105   intrinsically related to the amount of oxygen content during the synthesis. We succeeded

106   in controlling the transport properties of SnSe single crystals by changing the oxygen

107   amount presented in raw Sn as a surface oxidization. The electrical conducting behavior

108   varied from semiconductor to metal with increase of oxygen amount.

109

112   ‡Corresponding author: Aichi Yamashita

113   E-mail: YAMASHITA.Aichi@nims.go.jp

114   Postal address: National Institute for Materials Science, 1-2-1 Sengen, Tsukuba, Ibaraki

115   305-0047, Japan

116   Tel.: (+81)29-851-3354 ext. 2976

117

118

119   [1] H. Maier and D. R. Daniel, J. Electronic Materials **6**, 693 (1977)

120   [2] Martin Parenteau and Cosmo Carlone, Phys. Rev. B **41**, 5227 (1990)

121   [3] Takeshi Inoue, Hidenori Hiramatsu, Hideo Hosono, and Toshio Kamiya, J. Appl. Phys.

122   118, 205302 (2015)

123   [4] Li-Dong Zhao, Shih-Han Lo, Yongsheng Zhang, Hui Sun, Gangjian Tan, Ctirad

124   Uher, C. Wolverton, Vinayak P. Dravid & Mercouri G. Kanatzidis, Nature **508**, 373

125   (2014)

126   [5] Li-Dong Zhao, Gangjian Tan, Shiqiang Hao, Jiaqing He, Yanling Pei, Hang Chi, Heng

127   Wang, Shengkai Gong, Huibin Xu, Vinayak P. Dravid, Ctirad Uher, G. Jeffrey Snyder,

128   Chris Wolverton, Mercouri G. Kanatzidis, Science **351**, 6269 (2015)

129   [6] Yajie Fu, Jingtao Xu, Guo-Qiang Liu, Jingkai Yang, Xiaojian Tan, Zhu Liu, Haiming

130   Qin, Hezhu Shao, Haochuan Jiang, Bo Liang, and Jun Jiang, J. Mater. Chem. C, **4**,

131   1201 (2016)

132   [7] J. C. Li, D. Li, X.Y. Qina, J. Zhang, Scripta Materialia **126**, 6–10, (2017)

133   [8] Yi Li, Bin He, Joseph P. Heremans, Ji-Cheng Zhao, Journal of Alloys and

134   Compounds **669**, 224 (2016)

135   [9] Yulong Li, Xun Shi, Dudi Ren, Jikun Chen, and Lidong Chen, Energies, **8**, 6275

136   (2015)

137   [10] Xue Wang, Jingtao Xu, Guoqiang Liu, Yajie Fu, Zhu Liu, Xiaojian Tan, Hezhu

138   Shao, Haochuan Jiang, Tianya Tan , and Jun Jiang, Appl. Phys. Lett. **108**, 083902

139   (2016)

140   [11] Guodong Tang, Qiang Wen, Teng Yang, Yang Cao, Wei Wei, Zhihe Wang, Zhidong

141   Zhangb and Yusheng Li, RSC Adv., **7**, 8258 (2017)

142   [12] Eyob K. Chere, Qian Zhang, Keshab Dahal, Feng Cao, Jun Mao, and Zhifeng Ren,

143   J. Mater. Chem. A, **4**, 1848(2016)

144   [13] Qian Zhang, Eyob Kebede Chere, Jingying Sun, Feng Cao, Keshab Dahal, Shuo

145   Chen, Gang Chen, and Zhifeng Ren, Adv. Energy Mater., **2015**, 1500360 (2015)

146   [14] Hongliang Liu, Xin Zhang, Songhao Li, Ziqun Zhou, Yanqin Liu, and Jiuxing

147   Zhang, Journal of Electronic Materials, **46**, (2017)

148   [15] M. Gharsallah, F. Serrano-Sánchez, N. M. Nemes, F. J. Mompeán, J. L. Martínez,

149   M. T. Fernández-Díaz, F. Elhalouani & J. A. Alonso, Scientific Reports **6**, 26774

150   (2016)

151   [16] Anh Tuan Duong, Van Quang Nguyen, Ganbat Duvjir, Van Thiet Duong, Suyong

152   Kwon, Jae Yong Song, Jae Ki Lee, Ji Eun Lee, SuDong Park, Taewon Min,

153   Jaekwang Lee, Jungdae Kim & Sunglae Cho, Nature Communications **7**, 13713

154   (2016)

155   [17] Kunling Peng, Xu Lu, Heng Zhan, Si Hui, Xiaodan Tang, Guiwen Wang, Jiyan Dai,

156   Ctirad Uher, Guoyu Wang, Xiaoyuan Zhou, Energy and Environmental Science, **9**,

157   454-460 (2016)

158   [18] Cheng-Lung Chen, Heng Wang, Yang-Yuan Chen, Tristan Day, G. Jeffrey Snyder, J.

159   Mater. Chem. A, **2**, 11171-11176, (2014)

160   [19] D. Ibrahim, J.-B. Vaney, S. Sassi, C. Candolfi, V. Ohorodniichuk, P. Levinsky, C.

161   Semprimoschnig, A. Dauscher, and B. Lenoir, Appl. Phys. Lett. **110**, 032103

162   (2017)

163   [20] F. Serrano-Sánchez, M. Gharsallah, N. M. Nemes, F. J. Mompean, J. L. Martínez,

164   and J. A. Alonso, Appl. Phys. Lett. **106**, 083902 (2015)

165   [21] Niraj Kumar Singh, Sivaiah Bathula, Bhasker Gahtori, Kriti Tyagi, D. Haranath,

166 Ajay Dhar, Journal of Alloys and Compounds, **668**, 152-158, (2016)

167 [22] S. Sassi, C. Candolfi, J.-B. Vaney, V. Ohorodniichuk, P. Masschelein, A. Dauscher,

168 and B. Lenoir, Appl. Phys. Lett. **104**, 212105 (2014)

169 [23] Tian-Ran Wei, Chao-Feng Wu, Xiaozhi Zhang, Qing Tan, Li Sun, Yu Pan and

170 Jing-Feng Li, Phys. Chem. Chem. Phys., **17**, 30102-30109, (2015)

171 [24] L. Kövér, Zs. Kovács, R. Sanjinés, G. Moretti, I. Cserny, G. Margaritondo,

172 J. Pálinkás, H. Adachi, Surface and Interface Analysis, **23**, 461-466, (1995)

173

174

175   Fig. 1 (Color online) Sn $3d_{5/2}$ XPS spectrum for the surface of grain and powder Sn.
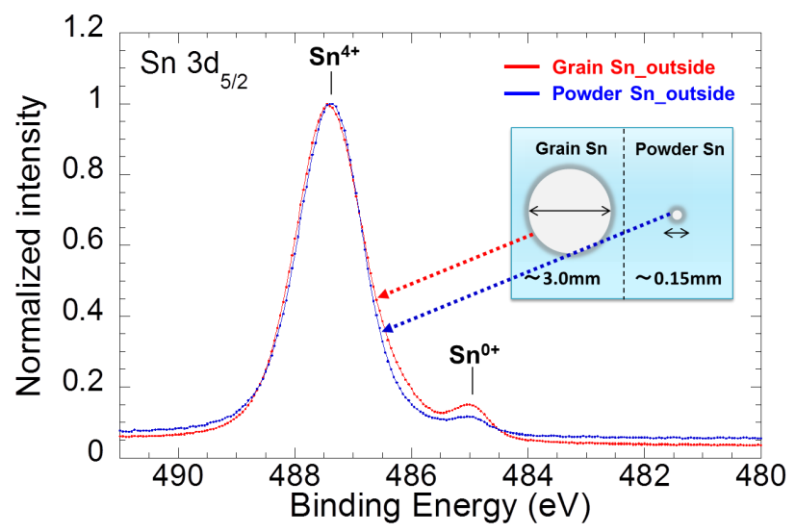
176   Fig. 2 (Color online) XRD patterns of the pulverized SnSe single crystals synthesized

177   from grain and powder Sn.

178   Fig. 3 (Color online) Temperature dependence of the electrical conductivity of SnSe

179   single crystals along the *bc*-plane grown by using different ratio of grain and powder form
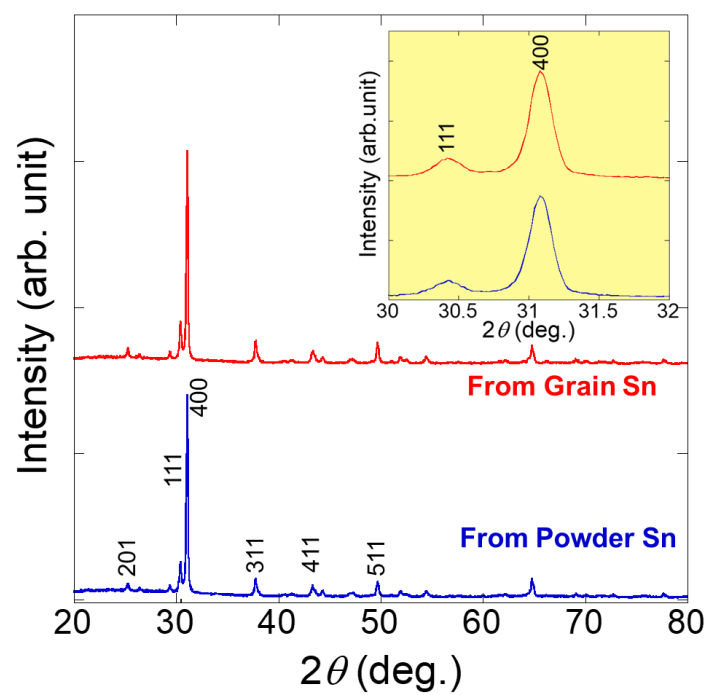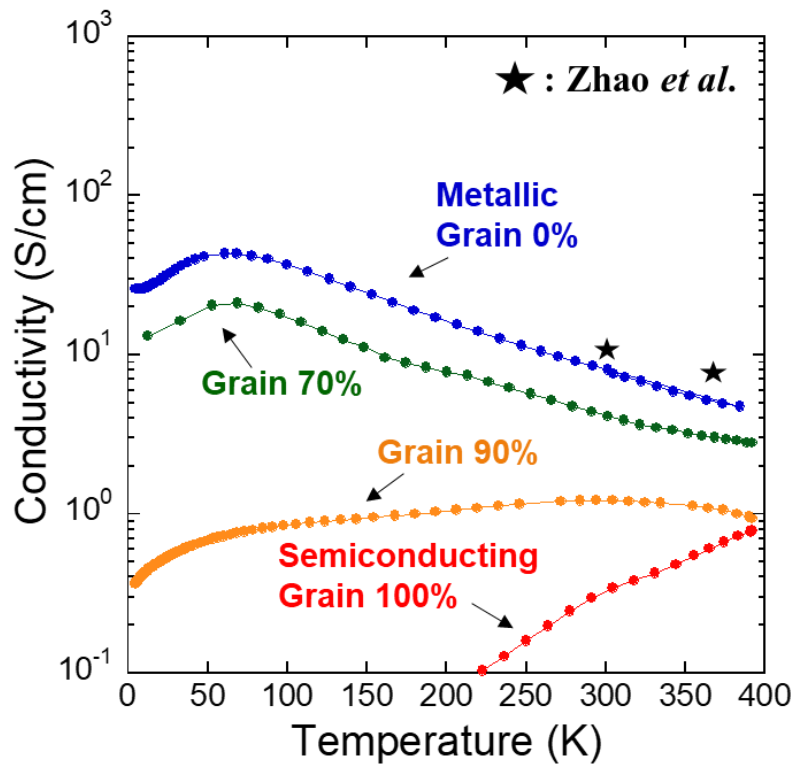
180   Sn as a starting material.

181

182 Fig.1

183

184

185 Fig.2

186

187

188

189

190   Fig.3